Volume 1 | Number 1 | Jan 2013 | Pages 1–100

# PCCP

Physical Chemistry Chemical Physics
www.rsc.org/pccp

ROYAL SOCIETY OF CHEMISTRY

ROYAL SOCIETY OF CHEMISTRY

www.rsc.org/pccp

# The Effect of Cations on $NO_2$ Production from the Photolysis of Aqueous Thin Water Films of Nitrate Salts

Nicole K. Richards-Henderson[1,2], Crisand Anderson[1], Cort Anastasio[2], and Barbara J. Finlayson-Pitts[1*]

[1]Department of Chemistry, University of California, Irvine, CA 92697-2025, USA. E-mail: bjfinlay@uci.edu; Fax: 949-824-2420; Tel: 949-824-7670
[2]Department of Land, Air and Water Resources, University of California - Davis, 1 Shields Ave., Davis, CA 95616, USA

Revision for:

*Physical Chemistry Chemical Physics*

Oct. 20, 2015

*Author to whom correspondence should be addressed. B.J. Finlayson-Pitts, (949)824-7670, e-mail bjfinlay@uci.edu

Cation_Nitrate_Oct20.doc

1

## Abstract

The photochemistry of nitrate ions in bulk aqueous solution is well known, yet recent evidence suggests that the photolysis of nitrate may be more efficient at the air-water interface. Whether and how this surface enhancement is altered by the presence of different cations is not known. In the present studies, thin aqueous films of nitrate salts with different cations were deposited on the walls of a Teflon chamber and irradiated with 311 nm light at 298 K. The films were generated by nebulizing aqueous 0.5 M solutions of the nitrate salts and the generation of gas-phase $NO_2$ was monitored with time. The nitrate salts fall into three groups based on their observed rate of $NO_2$ formation ($R_{NO2}$): (1) $RbNO_3$ and $KNO_3$, which readily produce $NO_2$ ($R_{NO2} > 3$ ppb min$^{-1}$), (2) $Ca(NO_3)_2$, which produces $NO_2$ more slowly ($R_{NO2} < 1$ ppb min$^{-1}$), and (3) $Mg(NO_3)_2$ and $NaNO_3$, which lie between the other two groups. Neither differences in the UV-visible spectra of the nitrate salt solutions nor the results of bulk-phase photolysis studies could explain the differences in the rates of $NO_2$ production between these three groups. These experimental results, combined with some insights from previous molecular dynamic simulations and vibrational sum frequency generation studies, show that cations may impact the concentration of nitrate ions in the interface region, thereby directly impacting the effective quantum yields for nitrate ions.
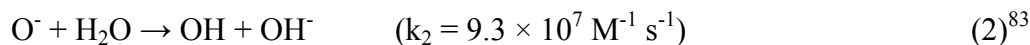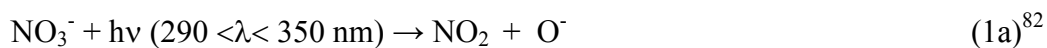
2

## 1. Introduction

The conventional view of simple salt solutions has been that ions are repelled from the air-water interface and prefer bulk solvation.[1] However, a combination of computational[2-16] and experimental studies[16-33] has shown that ions can reside and even be enhanced at the interface. The presence of ions at the interface has significant impacts on the chemistry in atmospheric aerosols, and on environmental surfaces, where interfacial ions can be oxidized at the surface without the need for gaseous oxidants to diffuse into the bulk.[15, 16] There is also evidence that the photolysis of species at the interface has higher quantum yields than those in the bulk.[34-48] In short, interfacial kinetics and mechanisms may be significantly different compared to those in the bulk phase.

The role of cations in the composition of the interface of aqueous solutions has not been studied directly but there has been substantial computational work on the effects of these ions on the organization of water molecules. Monte Carlo simulations by Hribar et al.[49] determined that large cations with low charge densities, e.g., $K^+$ and $Rb^+$, result in the surrounding water molecules being hydrogen bonded, whereas smaller ions, e.g., $Na^+$ and $Li^+$, with accompanying higher charge densities can break the hydrogen bonded network. This is consistent with ab initio calculations that show that smaller cations more strongly interact with water molecules,[50] and was confirmed by molecular dynamic (MD) simulations that show coordination numbers of water molecules increase around cations with increasing size.[51] Though computational studies have clearly shown that cations can alter surrounding water molecules, it is not well established whether cations can also affect chemical processes through effects on the concentration of anions at the air-water interface.

3

Nitrate ions are a common constituent of sea salt aerosols (100 – 400 mM)[52] due to oxidation of surface halide ions by oxides of nitrogen ($N_2O_5$, $NO_2$, $NO_3$ and $ClONO_2$),[53-81] as well as uptake of nitric acid from the gas phase.[81] Nitrate ions photolyze with actinic radiation, producing $NO_2$ and OH via (1a) and (2), and $NO_2^-$ and $O(^3P)$ through (1b).

$$NO_3^- + h\nu \ (290 < \lambda < 350 \text{ nm}) \rightarrow NO_2 + O^- \qquad\qquad (1a)^{82}$$

$$\rightarrow NO_2^- + O(^3P) \qquad\qquad (1b)^{82}$$

$$O^- + H_2O \rightarrow OH + OH^- \qquad (k_2 = 9.3 \times 10^7 \text{ M}^{-1} \text{ s}^{-1}) \qquad\qquad (2)^{83}$$

Molecular dynamics simulations,[45, 84-86] surface sensitive spectroscopy studies,[21, 33, 87-89] and surface tension measurements[6, 85] have been used to examine nitrate ions in solution, and most have concluded that in bulk aqueous solutions of $NaNO_3$ ($\geq$ 300 water molecules), nitrate is not in surface excess compared to the bulk. In bulk nitrate ion photolysis, $O^-$ and $NO_2$ formed via reaction (1a) have a high recombination rate due to solvent cage effects, thus regenerating nitrate ion.[82] Only photolysis products that escape the solvent cage are able to either escape into the gas-phase or diffuse into the bulk of solution. At room temperature the bulk-phase quantum yields are ~0.01 for OH production and an order of magnitude lower (~ 0.001) for $O(^3P)$ formation (1b) at 305 nm.[82, 90-93] In smaller water clusters (32-300 water molecules),[86] $NO_3^-$ ions are predicted to be present at the air-water interface. In the interface region, nitrate ions are less solvated than those in the bulk,[86] resulting in increased $NO_2$ production yields.[33, 46-48, 94]

Computational modeling and X-ray photoelectron spectroscopy show that cations ($Na^+$ and $Rb^+$) have a strong impact on $Br^-$ surface enhancement, affecting the ion's partitioning of halide ions

4

at the interface.[32]   Though $NO_3^-$ prefers bulk solvation compared to halide ions, $NO_3^-$ has similar

size and molecular polarizability as $Br^-$,[45] and its interfacial concentration and photochemistry

could be affected by the nature of the counter cation.   Recent vibrational sum frequency

generation measurements (VSFG) on aqueous nitrate salts determined that cations are less

surface active relative to the $NO_3^-$ ion and that the surface propensity of $NO_3^-$ is dependent on the

magnitude of the electric field between the cation and $NO_3^-$.[88, 95]     This paper is directed to

elucidating the impact cations have on nitrate ion photolysis in thin films of aqueous aerosols

deposited on a Teflon substrate by monitoring $NO_2$ production.

## 2. Experimental

*2.1 Thin Film Photolysis Studies*

The nitrate salts examined are represented by $MNO_3$, where M = $Na^+$, $Ca^{2+}$, $Mg^{2+}$, $K^+$, or $Rb^+$

(and divalent cations have two nitrates ions per mole of salt). 0.5 M $NO_3^-$ solutions (i.e.

monovalent $NO_3^-$ solutions are 0.5 M and divalent $NO_3^-$ solutions are 0.25 M) were aerosolized

into 70-L Teflon reaction chambers constructed with 51 μm thick FEP Teflon film using a 6-jet

Collison nebulizer (BGI Inc., Model CN25) at a backing pressure of 20 psi with $N_2$ (Oxygen

Service Co., UHP, 99.999%).   This process was repeated three times for 10 minutes each.

Suspended aerosol was evacuated each time, leaving a thin coating of aerosol on the inner walls

of the chamber.   The number of moles of $NO_3^-$ added to each chamber for each cation-nitrate

solution was assumed to be the same because the same amount of $MNO_3$ solution was

aerosolized into the chamber.   To ensure that the pumping out process did not result in

significant differences in aerosol coating the mass of aerosol for $NaNO_3$ on the walls was

determined to be 2.8  ± 0.4 grams (± 2s, n =3), for discussion of this calculation refer to Richards

5

et al. 2011.More details for coating the Teflon reaction chambers with salt solutions is described in detail elsewhere.[96]

The coated chambers were then filled with synthetic air (Scott-Marrin Inc., $NO_x < 0.001$ ppm, $SO_2 < 0.001$ ppm, Riverside, CA) that flowed through a water bubbler and mixed with dry air to adjust the final relative humidity (RH). For each $MNO_3$ experiment (except for $KNO_3$), the RH in the chamber was ~5% above the deliquescence relative humidity (DRH) of that salt (Table 1) so that the salts were aqueous solutions. In the $KNO_3$ system it was difficult to obtain reproducible and stable water vapor concentrations above 90% RH, so the experiments with $KNO_3$ were performed at 85%, below the DRH of $92.2 \pm 0.4\%$.

To the best of our knowledge, there are no reported literature values for the DRH of $RbNO_3$. The DRH of $RbNO_3$ was therefore measured experimentally by placing a saturated $RbNO_3$ solution in a humidity calibrator (Vaisala, HMK15) and sampling with a relative humidity-temperature probe (Vaisala, HMP 338) every hour until three consistent measurements were obtained to ensure equilibration and reproducibility.

Irradiation of the thin aqueous salt film on the walls of the Teflon chamber was carried out using eight externally mounted narrowband UVB lamps ($\lambda_{max} \sim 311$ nm) which overlap with the nitrate $n \rightarrow \pi^*$ absorption band. The reaction chamber is actively cooled using an external fan to prevent dehydration of the film. All experiments were conducted at $298 \pm 2$ K. The $NO_2$ concentrations were monitored as a function of time by periodically sampling with a chemiluminescence nitrogen oxides analyzer (ThermoElectron Corp., Model 42C). Calibration

6

of the nitrogen oxides analyzer was performed using known mixtures of $NO_2$ (4.57 ppm; Scott Marrin Inc.) or NO in $N_2$ at levels similar to those detected during photolysis.

## 2.2 UV/Visible Spectra

The UV absorption spectrum was taken for each $MNO_3$ at 0.5 nm resolution using a Cary 50 UV – visible spectrophotometer for nitrate ion concentrations of 0.5 M and 2 M using a 1 cm and 0.1 cm UV-visible grade quartz cell, respectively.

## 2.3 Bulk Photolysis Studies

The formation rates of OH from $NO_3^-$ photolysis were measured in bulk $MNO_3$ solutions by adding benzene as a chemical probe and measuring the stable product phenol.    Benzene was chosen as the chemical probe because it has been previously proven useful for trapping OH,[97] does not have a counter cation and will not affect solution pH.    Air-saturated solutions of 5.0 mM $MNO_3$ and 10.0 mM benzene were placed in an airtight 2-cm, far-UV, quartz cuvette (Spectrocell), placed in a temperature-controlled illumination chamber at 298 K with continuous stirring and illuminated with 313 nm light from a monochromatic illumination system with a 1000 W Hg/Xe lamp.  For each illumination experiment, a dark control (with corresponding rate of phenol formation $R_{dark}$) was also performed, consisting of a quartz cell wrapped in aluminum foil and treated identically (sample composition and temperature) as the illuminated sample.  On each day of experiments, two measurements were also performed: (1) a blank control containing benzene only (with corresponding phenol rate $R_{blank}$) and (2) measurement of the photon flux in the chamber using 10 μM 2-nitrobenzaldehyde (2NB) as a chemical actinometer to test for possible lamp intensity fluctuations.[98]   The rate of photolysis of 2NB did not differ significantly from day to day ($J_{2NB}= (7.1 \pm 0.3) \times 10^{-3}$ s$^{-1}$).  Aliquots of sample were removed from the quartz

7

cells at measured time intervals during illumination and the phenol concentration was measured using high performance liquid chromatography (HPLC). The HPLC system consisted of a Shimadzu SPD-10A UV-Vis detector, LC-10AT pump, and a $250 \times 33$ mm, 5 μM bead, BetaBasic-18 column (Thermo Hypersil-Keystone). The HPLC eluent was 30:70 acetonitrile-water mixture at a flow rate of 0.5 ml min$^{-1}$.

For each experimental day, the HPLC was calibrated with aqueous phenol standards to span the range of values detected. The rate of phenol formation, $R_{Phen}$, during illumination was determined from plots of phenol concentrations versus illumination time using a linear regression. Rates of phenol formation in dark or blank samples were $\leq 1\%$ of the sample value. The measured $R_{Phen}$ was converted to the rate of OH formation, $R_{OH}$, by dividing by the yield of phenol formed from the reaction of OH with benzene ($Y_{Phen} = 0.69$).[97]

For the majority of experiments, the benzene concentration was 10.0 mM which was sufficiently high to trap all of OH generated from the 5.0 mM MNO$_3$ solutions. To determine the benzene concentration needed to trap all of the generated OH, separate experiments at either constant concentrations of NaNO$_3$ or Mg(NO$_3$)$_2$ with varied benzene concentrations were conducted (Fig. S1). For both of these sets of experiments, the rate of phenol formation increased with increasing benzene concentration until the concentration ratio [benzene]:[NO$_3^-$] $\geq 1$, at which point the rate remained constant, indicating that all of the OH was scavenged. Solutions were typically at a pH of $5.1 \pm 0.2$ (unadjusted) with a less than $\pm 0.3$ change in pH by the end of illumination.

8

*2.4 Error Analysis*

All errors are reported as 2s, where s is the sample standard deviation, defined as

$$s = \sqrt{\frac{(\sum_{i=1}^{N}(x_i - \bar{x})^2)}{N-1}}$$  (eq. 1)

where $N$, the number of samples, was 3-5, depending on the measurement.[99]

*2.5 Chemicals*

The salts NaNO$_3$ (Fischer Scientific, 99.4%), KNO$_3$ (Fisher, >99.4%), RbNO$_3$ (Fluka, 99%), Ca(NO$_3$)$_2$·4H$_2$O (Fluka, 99.0%) and Mg(NO$_3$)$_2$·6H$_2$O (Sigma-Aldrich, 98.0%) were used as received from the manufacturers and 0.50 M nitrate ion solutions were made from each using Milli-Q water (18.2 M$\Omega$ cm). Sodium benzoate ($\geq$99.0%), benzene ($\geq$99.7%), and phenol ($\geq$99%) were purchased from Sigma Aldrich.

## 3. Results and Discussion

Figure 1 shows the formation of NO$_2$ as a function of illumination time (Fig.1a) and the corresponding rates of NO$_2$ production ($R_{NO2}$, Fig. 1b) during the illumination of thin films containing NO$_3^-$ with different cations: Na$^+$, K$^+$, Rb$^+$, Ca$^{2+}$ and Mg$^{2+}$. All experiments with the exception of KNO$_3$ were conducted at 5% above the deliquescence relative humidity (DRH, Table 1) so that the salts were aqueous solutions, which was confirmed by visual inspection.

As mentioned in the experimental section, the experiments for KNO$_3$ were performed just under the DRH, at 85%. To gain added insight into how this might affect the rate of NO$_2$ production, photolysis of NaNO$_3$ was studied as a function of relative humidity above and below the deliquescence point (Fig. 2). Above the DRH (73.8% for NaNO$_3$), there is no more than a 15%

difference in the $R_{NO2}$.   This is consistent with water activity measurements by Tang and Munkelwitz[100] in which the concentration of $NO_3^-$ was shown to change by only ~18% for $NaNO_3$ aerosols with RH ranging from 75-87%.   Since the photolysis rate is independent of nitrate concentration but dependent on the moles of $NO_3^-$ (see SI), the increased water (and film volume) at higher relative humidity has only a minor effect on the rate of nitrate photolysis.   In the range of 50 - 75% RH, below the DRH of $NaNO_3$, $NO_2$ continues to be generated but at a smaller rate.   While the salt is solid under these conditions, it holds significant amounts of surface-adsorbed water [101-104] which increases ion mobility at the interface and provides some liquid-like character to the surface.   These results for $NaNO_3$ suggest that $R_{NO2}$ from $KNO_3$ would be higher if photolysis experiments were conducted 5% above the DRH rather than 7% below, and hence the data in Fig 1 for $KNO_3$ represent lower limits.

Values of the $R_{NO2}$ in Fig. 1 fall into three groups: (1) $RbNO_3$ and $KNO_3$, which rapidly photolyze to form $NO_2 > 3$ ppb min$^{-1}$), (2) $Ca(NO_3)_2$, which photolyzes more slowly ($R_{NO2} \leq 1$ ppb min$^{-1}$), and (3) $Mg(NO_3)_2$ and $NaNO_3$, which have intermediate rates. The difference in the $R_{NO2}$ between these groups is unexpected because the only difference is the counter cation. Cations have been generally thought to be spectator ions, and are believed to play a minor role in both chemical and photochemical processes.

One potential source of difference between the cation-nitrate salts could be that they possess different UV absorption spectra, resulting in more rapid photolysis of $RbNO_3$ and $KNO_3$ compared to $Mg(NO_3)_2$, $NaNO_3$ and $Ca(NO_3)_2$.   To probe this possibility, the UV-visible absorption spectra of aqueous $MNO_3$ solutions (0.5 M and 2 M) were measured (Fig. S2).   The

10

molar absorptivies of the $MNO_3$ salts for both 0.5 M and 2 M are all centered around $302 \pm 1$ nm, and do not vary significantly between the different salts, suggesting that changes in the absorption spectra cannot be responsible for the increase in the $R_{NO2}$ for the different cation-nitrate salts. However, studies by Hudson et al.[105] showed that as $Ca(NO_3)_2$, $Mg(NO_3)_2$, and $NaNO_3$ become more concentrated, the lowest electronic absorption (n $\rightarrow \pi^*$) shifts to shorter wavelengths and decreases in intensity. From their results, $Ca(NO_3)_2$ showed the largest change in light absorption, with a 10% decrease from 0.5 M to 5.8 M. These minor changes suggest that differences in the absorption spectra cannot account for the large differences in the $R_{NO2}$ between $MNO_3$. Even though concentrations in the thin films do change depending on RH, this should not affect the photolysis rate since there was no significant light attenuation in the thin films (see calculation in SI).

Another possibility to explain the photolysis differences between the different salts (Figure 1) is that there could be a bulk-phase photochemical process in which cations disrupt the solvent cage around nitrate ions, allowing photolysis products to more easily escape. However, one photolysis study of bulk nitrate solutions[106] reported that the quantum yield of $NO_2^-$ formation via reaction *1b* was not sensitive to the nature of the counter ion. As illustrated in reaction *1a* and *1b*, $NO_2$ and $NO_2^-$ are both products of $NO_3^-$ photolysis and therefore we would expect that if cations were affecting the solvent cage in the bulk, then the $NO_2^-$ and OH yields would be affected as well. To verify that a bulk-phase process does not affect nitrate photolysis, bulk-phase OH solution measurements were performed by following phenol production with time. Figure 3 shows that the $R_{OH}$ is not statistically different between the five $MNO_3$ salts, with an average value of $1.9 \pm 0.08$ $\mu M$ $min^{-1}$. The corresponding average value of $\Phi(OH)$ is $(1.1 \pm 0.4)$

$\times\ 10^{-2}$ (see Chu and Anastasio[97] for details of the calculation), which agrees well with past studies reporting a value of $\sim 0.01$ at room temperature.[82, 90-93, 97]

These OH experiments thus suggest that the nature of the cations is not influencing the production of nitrate photo-products in the bulk. However, the bulk-phase measurements were conducted at concentrations that were a factor of 600 (for $RbNO_3$) to 2040 (for $NaNO_3$) times lower than the thin film experiments due to the low solubility of benzene in aqueous solution (23 mM). Thus there is a possibility that a higher $R_{OH}$ would result in the bulk studies if experiments could be conducted at higher nitrate ion concentrations. To test this, the influence of nitrate ion concentration on the $\Phi(OH)$ in the bulk-phase was determined using $NaNO_3$, which has the largest concentration difference between the bulk and thin film photolysis experiments. In this case, sodium benzoate was used as the chemical probe due to its much larger solubility in water compared to benzene (4240 mM), allowing for nitrate ion concentrations closer to those in the thin-film experiments to be used. The $\Phi(OH)$ was found to be independent of nitrate ion concentrations between 0.05 mM to 0.5 M, with an average value of $(1.0 \pm 0.5) \times 10^{-2}$ (Fig. S3).

The absence of a bulk-phase explanation suggests that cations may be affecting the partitioning of $NO_3^-$ near the surface, where an incomplete solvent cage enhances photo-product formation. The observed $R_{NO2}$ can be expressed as a combination of contributions from the interface region and the bulk:

$$R_{NO2} = I_\lambda * \sigma_\lambda\ (\phi^{int} \times N^{int} + \phi^b \times N^b) \qquad \text{(eq. 2)}$$

In eq. 2, $I_\lambda$ is the photon flux from the narrow-band UVB lamps, $\sigma_\lambda$ is the absorption cross-section of $NO_3^-$, $\phi^{int}$ and $\phi^b$ are the quantum yields for $NO_2$ formation from $NO_3^-$ photolysis in the interface region and the bulk, respectively, and $N^{int}$ and $N^b$ are the number of available nitrate ions in each region. Given that the same number of moles of $NO_3^-$ was added into each reaction chamber, the amount of nitrate in the bulk will be the same for each $MNO_3$. Similarly, the bulk quantum yields for the different salts are the same (Figure 3). Therefore, this suggests that the first term ($\phi^{int} \times N^{int}$) is responsible for the observed differences in the rates of production of $NO_2$.

To assess if interfacial chemistry is responsible for the observed change in $R_{NO2}$, a combination of our experimental data and previous MD simulations was used. Assuming that bulk nitrate photochemistry dominates $NO_2$ release from $NaNO_3$, the ratio of the $R_{NO2}$ production for $KNO_3$ ($R_{NO2}^K$) to $NaNO_3$ ($R_{NO2}^{Na}$) can be expressed as a combination of contributions from the interface region and the bulk (eq. 3):

$$\frac{R_{NO2}^K}{R_{NO2}^{Na}} = \frac{[\phi_K^{int} N_K^{int} + \phi_K^b N_k^b\ ]}{[\ \phi_{Na}^b N_{Na}^b\ ]} \qquad\qquad \text{(eq. 3)}$$

It is assumed that the interface region for $NaNO_3$ does not contribute significantly to the production of $NO_2$ because of the relatively small concentrations of nitrate ions near the interface. Eq. 3 can be rewritten in the form of eq. 4:

$$\frac{R_{NO2}^K}{R_{NO2}^{Na}} = \frac{\phi_K^{int} N_K^{int}}{\phi_{Na}^b N_{Na}^b} + \frac{\phi_K^b N_k^b}{\phi_{Na}^b N_{Na}^b} \approx \frac{\phi_K^{int} N_K^{int}}{\phi_{Na}^b N_{Na}^b} + 1 \qquad\qquad \text{(eq. 4)}$$

13

The second term in eq. 4 is taken to be ~1 since (a) the bulk-phase studies (Fig. 3) show that $\phi_K^b = \phi_{Na}^b$ and (b) equal amounts of nitrate were added to the chamber for both $NaNO_3$ and $KNO_3$, so the number of ions in the bulk (which forms most of the 800 nm thick film) is essentially the same; even in the case of enhancement of nitrate ions in the interface region for the potassium salt (see below), the interface layer (taken as 1 nm) is too small to affect the bulk-phase number significantly. Thus $\frac{N_k^b}{N_{Na}^b} \sim 1$ as well.

The measured ratio of the rates of gas-phase $NO_2$ production for the potassium salt compared to the sodium salt is $1.73 \pm 0.34$ (Fig. 1). Thus eq. 4 becomes:

$$\frac{\phi_K^{int} N_K^{int}}{\phi_{Na}^b N_{Na}^b} = 0.73 \qquad \text{(eq. 5)}$$

Rearranging this to solve for $\phi_K^{int}$ gives

$$\phi_K^{int} = 0.73 \frac{\phi_{Na}^b N_{Na}^b}{N_K^{int}} \qquad \text{(eq. 6)}$$

If nitrate ions were equally distributed over the interface and bulk regions, i.e., there was no enhancement of $NO_3^-$ at the $KNO_3$ interface compared to in the $NaNO_3$ bulk, then $\frac{N_K^{int}}{N_{Na}^b} = \frac{1}{799}$. Applying this value and the bulk phase $\phi_{Na}^b$ =0.011 in eq. 6 gives $\phi_K^{int}$ = 6.4. Since the quantum yield for $NO_2$ production must be $\leq 1.0$, this is not reasonable and suggests that some combination of enhancement of nitrate ions at the interface for the $KNO_3$ salt (relative to

14

NaNO$_3$) and an enhancement in the quantum yield at the interface over that for the bulk must be occurring.

The results of previous MD simulations suggest that the nitrate ion concentrations in the interface region, although smaller than in the bulk, are a factor of 10 higher for KNO$_3$ compared to NaNO$_3$.[45, 47] This factor arises from the fraction of nitrate ions at the interface determined from the integrated density profile area of NO$_3^-$ within $\pm$ 0.5 nm of the GDS; for a 2 M KNO$_3$ solution the ratio of the number of nitrate ions in the interface region compared to that in the bulk is 0.3 and the corresponding number for 2 M NaNO$_3$ is 0.03. Taking this relative increase in nitrate concentration in the KNO$_3$ interface region into account (example calculation provided in SI), the calculated quantum yield at the interface drops to 0.6 $\pm$ 0.2. There are several uncertainties in this quantum yield calculation. These include: (1) since the $R_{NO2}$ measurement for KNO$_3$ was conducted below the DRH, it might be an underestimate (i.e., $\phi_K^{int}$ might be higher), and (2) the calculation assumes a "baseline" ratio of $\frac{N_K^{int}}{N_{Na}^b} = \frac{1}{799}$ (based on an assumed equal distribution throughout the films), but this is not constrained by measurements or modeling. Despite the uncertainties, the calculated interfacial quantum yield for KNO$_3$ is much larger than the bulk quantum yield of 0.011, emphasizing that cations play a strong role in the ion organization and photochemistry in thin films. In this case, interfacial nitrate accounts for roughly 40% of NO$_2$ production from KNO$_3$ photolysis, compared to 7% for the NaNO$_3$ films (see calculation in Supporting Information).

MD simulations also show that 2 M Mg(NO$_3$)$_2$[85] has a ratio of 0.2 in the number of nitrate ions in the interface region compared to the bulk, resulting in a factor increase of 7 more NO$_3^-$ in the

interface region compared to NaNO$_3$. It would therefore be expected that the rate of NO$_2$ production would also be higher for the magnesium salt compared to the sodium salt and that the order for $R_{NO2}$ would be KNO$_3$ > Mg(NO$_3$)$_2$ > NaNO$_3$, consistent with data in Fig. 1. The measured value for $R_{NO2}$ from Mg(NO$_3$)$_2$ is about 10% higher than NaNO$_3$ (ratio is 1.1 ± 0.2), but using eq. 4 and assuming an interfacial quantum yield of 0.6, the expected ratio $\frac{R_{NO2}^{Mg}}{R_{NO2}^{Na}}$ is 1.5 ± 0.2. However, given the experimental error, definitive conclusions cannot be drawn. MD simulations are not available in the literature for RbNO$_3$ and Ca(NO$_3$)$_2$, which precluded carrying out similar comparisons.

Recent VSFG studies for divalent cations have shown that at the air-aqueous interface columbic cation-nitrate interactions do change depending on the cation.[95] For example, Ca$^{2+}$ nitrate solutions showed considerably more contact-ion pairing (with no solvent molecules between ions) compared to Mg$^{2+}$. This resulted in Mg(NO$_3$)$_2$ having 50% more free nitrate ions at the air-water interface compared to Ca(NO$_3$)$_2$. As shown in Fig. 1, the $R_{NO2}$ for Mg(NO$_3$)$_2$ is approximately 2.9 times faster than Ca(NO$_3$)$_2$. Therefore, one possibility is that free nitrate at the interface may photolyze more efficiently than cation-nitrate ion pairs at the interface.

## 4. Conclusions

This study shows that the rate of production of gas-phase NO$_2$ from thin films of nitrate salts is enhanced for RbNO$_3$ and KNO$_3$, somewhat less for Mg(NO$_3$)$_2$ and NaNO$_3$ and even less for Ca(NO$_3$)$_2$. Neither differences in the UV-visible spectra of the aqueous solutions of the salts,

16

nor changes in bulk-phase photolysis for the different salt solutions, are consistent with this enhancement.  Previous MD simulations and VSFG studies suggest that higher concentrations of nitrate ions at the air-water interface, especially those that do not have strong columbic attractions with their counter-cation, may explain this enhancement.  Thus cations can play a role in photochemical processes, possibly by changing the concentration of nitrate ions in the interface region.

## Acknowledgements

## Supporting Information

Figures showing the rate of OH formation for bulk nitrate solutions as a function of added benzene, UV/vis absorption spectra and the quantum yields of OH as a function of $NaNO_3$ solution concentration.

18

**Table 1:** Equilibrium saturation concentrations for nitrate ions in water at their deliquescence points

| Compound | Equilibrium saturation concentration (M)[107] | Deliquescence Point (%)[108] |
|---|---|---|
| $Mg(NO_3)_2 \bullet 6H_2O$ | 4.9 | 52.9 |
| $Ca(NO_3)_2 \bullet 4H_2O$ | 5.8 | 55.5 |
| $NaNO_3$ | 10.2 | 73.8 |
| $KNO_3$ | 3.3 | 92.2 |
| $RbNO_3$ | 3.0 | 85.2* |

*$RbNO_3$ was experimentally measured.

**Figure Captions**

**Figure 1:** (a) $NO_2$ production during photolysis experiments for aqueous thin films of $Ca(NO_3)_2$ (red, squares), $NaNO_3$ (orange, diamonds), $Mg(NO_3)_2$ (purple, circles), $KNO_3$ (green, diamonds) and $RbNO_3$(blue, triangles), and (b) the corresponding rates of $NO_2$ production at 298 K in air. Hatched bars and open symbols for $KNO_3$ denote experiments conducted below the DRH. Error bars are 2s of triplicate experiments.

**Figure 2:** Rates of $NO_2$ release in $NaNO_3$ photolysis experiments as a function of RH. The vertical dashed line is the $NaNO_3$ DRH. Error bars are 2s of duplicate experiments.

**Figure 3:** The rate of OH production in bulk-phase photolysis studies conducted at 313 nm and 298 K. Error bars are 2s of triplicate experiments.

References

1       L. Onsager and N. Samaras, *J. Chem. Phys.*, 1934, **2**, 528.
2       P. Jungwirth and D. Tobias, *J. Phys. Chem. B*, 2000, **104**.
3       P. Jungwirth and D. J. Tobias, *J. Phys. Chem. B*, 2001, **105**, 10468-10472.
4       P. Jungwirth and D. J. Tobias, *J. Phys. Chem. B*, 2002, **106**, 6361-6373.
5       P. Jungwirth and D. J. Tobias, *Chem. Rev.*, 2006, **106**, 1259-1281.
6       L. M. Pegram and M. T. Record, *Proc. Natl. Acad. Sci.* , 2006, **103**, 14278-14281.
7       L. X. Dang and T. M. Chang, *J. of Phys. Chem. B*, 2002, **106**, 235.
8       G. Archontis, E. Leontidis and G. Andreou, *J. Phys. Chem. B*, 2005, **109**, 17957-17966.
9       T. M. Chang and L. X. Dang, *Chem. Rev.*, 2006, **106**, 1305-1322.
10      T. Ishiyama and A. Morita, *J. Phys. Chem. C*, 2007, **111**, 721-737.
11      S. J. Stuart and B. J. Berne, *J. Phys. Chem.*, 1996, **100**, 11934-11943.
12      L. X. Dang, *J. Phys. Chem. B*, 2002, **106**, 10388-10394.
13      L. Perera and M. L. Berkowitz, *J. Chem. Phys.*, 1994, **100**, 3085.
14      L. S. Sremaniak, L. Perera, M. L. Berkowitz and *Chem. Phys. Lett.*, 1994, **218**, 377-382.
15      S. W. Hunt, M. Roeselová, W. Wang, L. M. Wingen, E. M. Knipping, D. J. Tobias, D. Dabdub and B. J. Finlayson-Pitts, *J. Phys. Chem. A*, 2004, **108**, 11559-11572.
16      E. M. Knipping, M. J. Lakin, K. L. Foster, P. Jungwirth, D. J. Tobias, R. B. Gerber, D. Dabdub and B. J. Finlayson-Pitts, *Science*, 2000, **288**, 301-306.
17      E. K. Frinak and J. P. D. Abbatt, *J. Phys. Chem. A.*, 2006, **110**, 10456-10464.
18      K. W. Oum, M. J. Lakin and B. J. Finlayson-Pitts, *Geophys. Res. Lett.*, 1998, **25**, 3923-3926.
19      D. Clifford and D. J. Donaldson, *J. of Phys. Chem. A.*, 2007, **111**, 9809-9814.
20      D. Liu, G. Ma, L. Levering and H. Allen, *J. Phys. Chem. B*, 2004, **108**, 2252.
21      C. Schnitzer, S. Baldelli and M. J. Shultz, *J. Phys. Chem. B*, 2000, **104**, 585-590.
22      S. Ghosal, J. C. Hemminger, H. Bluhm, B. S. Mun, E. L. D. Hebenstreit, G. Ketteler, D. F. Ogletree, F. Requejo and M. Salmeron, *Science*, 2005, **307**, 563-566.
23      M. Brown, R. D' Auria, I. Kuo, M. Krisch, D. Starr, H. Bluhm, D. Tobias and J. Hemminger, *Phys. Chem. Chem. Phys.*, 2008, **10**, 4778-4784.
24      N. Ottosson, M. Faubel, S. Bradforth, P. Jungwirth and B. Winter, *J. Electron Spectrosc. Relat. Phenom.*, 2010, **177**, 60-70.
25      P. B. Petersen and R. J. Saykally, *Chem. Phys. Lett.*, 2004, **397**, 51-55.
26      M. Mucha, T. Frigato, L. M. Levering, H. C. Allen, D. J. Tobias, L. X. Dang and P. Jungwirth, *J. of Phys. Chem. B*, 2005, **109**, 7617-7623.
27      J. Cheng, C. D. Vecitis, M. R. Hoffmann and A. J. Colussi, *J. Phys. Chem. B*, 2006, **110**, 25598-25602.
28      E. A. Raymond and G. L. Richmond, *J. Phys. Chem. B*, 2004, **108**, 5051-5059.
29      P. B. Petersen, J. C. Johnson, K. P. Knutsen and R. J. Saykally, *Chem. Phys. Lett.*, 2004, **297**, 46-50.
30      J. H. Hu, Q. Shi, P. Davidovits, D. R. Worsnop, M. S. Zahniser and C. E. Kolb, *J. Phys. Chem.*, 1995, **99**, 8768-8776.
31      A. Laskin, D. J. Gaspar, W. Wang, S. W. Hunt, J. P. Cowin, S. D. Colson and B. J. Finlayson-Pitts, *Science*, 2003, **301**, 340-344.

21

32    M. H. Cheng, K. M. Callahan, A. M. Margarella, D. J. Tobias, J. C. Hemminger, H. Bluhm and M. J. Krisch, *J. Phys. Chem. C*, 2012, **116**, 4545-4555.

33    A. C. Hong, S. N. Wren and D. J. Donaldson, *J. Phys. Chem. Lett.*, 2013, **4**, 2994-2998.

34    J. D. Graham, J. T. Roberts, L. D. Anderson and V. H. Grassian, *J. Phys Chem.*, 1996, **100**, 19551-19558.

35    A. Furlan, *J. Phys. Chem. B*, 1999, **103**, 1550-1557.

36    J. Vieceli, I. Chorny and I. Benjamin, *J. Chem. Phys.*, 2001, **115**, 4819-4828.

37    N. Winter and I. Benjamin, *J. Chem. Phys.*, 2004, **121**, 2253-2263.

38    P. Nissenson, C. J. H. Knox, B. J. Finlayson-Pitts, L. F. Phillips and D. Dabdub, *Phys. Chem. Chem. Phys.*, 2006, **8**, 4700-4710.

39    S. Khanra, C. Minero, V. Maurino, E. Pelizzetti, B. K. Dutta and D. Vione, *Environ. Chem. Lett.*, 2008, 29-34.

40    I. Benjamin, *J. Chem. Phys.*, 1991, **95**, 3698.

41    I. Chorny, J. Vieceli and I. Benjamin, *J. Phys. Chem. B*, 2003, **107**, 229-236.

42    A. Yabushita, T. Hama, D. Iida and M. Kawasaki, *J. Chem. Phys.*, 2008, **129**.

43    A. Yabushita, D. Iida, T. Hama and M. Kawasaki, *J. Phys Chem. A*, 2008, **112**, 9763-9766.

44    A. Yabushita, N. Kawanaka, M. Kawasaki, P. D. Hamer and D. E. Shallcross, *J. Phys. Chem. A*, 2007, **111**, 8629-8634.

45    J. L. Thomas, M. Roeselová, L. X. Dang and D. J. Tobias, *J. Phys. Chem. A*, 2007, **111**, 3091-3098.

46    N. K. Richards and B. J. Finlayson-Pitts, *Environ. Sci. Technol.*, 2012, **46**, 10447-10454.

47    N. K. Richards, L. M. Wingen, K. M. Callahan, N. Nishino, M. T. Kleinman, D. J. Tobias and B. J. Finlayson-Pitts, *J. Phys. Chem. A*, 2011, **115**   5810-5821.

48    N. K. Richards-Henderson, K. M. Callahan, P. Nissenson, N. Nishino, D. J. Tobias and B. J. Finlayson-Pitts, *Phys. Chem. Chem. Phys.*, 2013, **15**, 17636-17646.

49    B. Hribar, N. T. Southall, V. Vlachy and K. A. Dill, *J. Am. Chem. Soc.*, 2002, **124**, 12302.

50    P. A. Knollman and R. D. Kuntz, *J. Am. Chem. Soc.*, 1972, **94**, 9236-9237.

51    S. H. Lee and J. C. Rasaiah, *J. Chem. Phys.*, 1994, **101**, 6964.

52    C. Anastasio and J. T. Newberg, *J. Geophys. Res.*, 2007, **112**, D10306, doi: 10310.11029/12006JD008061.

53    R. C. Robbins, R. D. Cadle and D. L. Eckhardt, *J. Meteor*, 1959, **16**, 53-56.

54    R. D. Cadle and R. C. Robbins, *Discuss. Faraday Soc.*, 1960, **30**, 155-161.

55    W. H. Schroeder and P. Urone, *Environ. Sci. Technol.*, 1974, **8**, 756-758.

56    B. J. Finlayson-Pitts, *Nature*, 1983, **306**, 676-677.

57    C. Zetzsch, G. Pfahler and W. Behnke, *J. Aerosol Sci.*, 1988, **19**, 1203-1206.

58    B. J. Finlayson-Pitts, M. J. Ezell and J. N. Pitts Jr., *Nature*, 1989, **337**, 241-244.

59    W. Behnke and C. Zetzsch, *J. Aerosol Sci.*, 1989, **20**, 1167-1170.

60    W. Behnke and C. Zetzsch, *J. Aerosol Sci.*, 1990, **21**, S229-S232.

61    W. Behnke, H.-U. Kruger, V. Scheer and C. Zetzsch, *J. Aerosol Sci.*, 1991, **22**, S609-S612.

62    F. E. Livingston and B. J. Finlayson-Pitts, *Geophys. Res. Lett.*, 1991, **18**, 17-21.

63    T. Winkler, J. Goschnick and H. J. Ache, *J. Aerosol Sci.*, 1991, **22, Supplement 1**, S605-S608.

64    W. Behnke, V. Scheer and C. Zetzsch, *J. Aerosol Sci.*, 1994, **25**, 277-278.

65    I. M. Msibi, Y. Li, J. P. Shi and R. M. Harrison, *J. Atmos. Chem.*, 1994, **18**, 291.

22

66      J. M. Laux, J. C. Hemminger and B. J. Finlayson-Pitts, *Geophys. Res. Lett.*, 1994, **21**, 1623-1626.

67      F. F. Fenter, F. Caloz and M. J. Rossi, *J. Phys. Chem.*, 1996, **100**, 1008.

68      H. C. Allen, J. M. Laux, R. Vogt, B. J. Finlayson-Pitts and J. C. Hemminger, *J. Phys. Chem.*, 1996, **100**, 6371-6375.

69      R. Karlsson and E. Ljungström, *J. Aerosol Sci.*, 1995, **26**, 39-50.

70      C. D. Zangmeister and J. E. Pemberton, *J. Phys. Chem. B*, 1998, **102**, 8950.

71      A. Laskin, M. J. Iedema and J. P. Cowin, *Environ. Sci. Technol.*, 2002, **36**, 4948-4855.

72      E. E. Gard, et al., *Science*, 1998, **279**, 1184-1187.

73      M.-T. Leu, R. S. Timonen, L. F. Keyser and Y. L. Yung, *J. Phys. Chem.*, 1995, **99**, 13203-13212.

74      M. Gershenzon, S. Il'in, N. Fedotov, Y. Gershenzon, E. Aparina and V. Zelenov, *J Atmos Chem*, 1999, **34**, 119-135.

75      C. Zetzsch and W. Behnke, *Ber. Bunsen-Ges. Phys. Chem.*, 1992, **96**, 488-493.

76      C. Zetzsch and W. Behnke eds., *Heterogeneous Reactions of Chlorine Compounds*, Springer-Verlag, Berlin, 1993.

77      J. R. Arnold and W. T. Luke, *Atmos. Environ.*, 2007, **41**, 4227-4241.

78      M. J. Rossi, *Chem Rev.*, 2003, **103**, 4823-4882.

79      B. J. Finlayson-Pitts, *Chem. Rev.*, 2003, **103**, 4801-4822.

80      B. J. Finlayson-Pitts, *Anal. Chem.*, 2009, **82**, 770-776.

81      B. J. Finlayson-Pitts and J. N. Pitts, Jr., *Chemistry of the Upper and Lower Atmosphere - Theory, Experiments, and Applications*, Academic Press, San Diego, 2000.

82      J. Mack and J. R. Bolton, *J. Photochem. Photobiol. A Chem.*, 1999, **128**, 1-13.

83      G. V. Buxton, *Trans. Faraday Soc.*, 1970, **66**, 1656-1660.

84      L. X. Dang, T. M. Chang, M. Roeselová, B. C. Garrett and D. J. Tobias, *J. Chem. Phys.*, 2006, **14**, 066101.

85      B. Minofar, R. Vacha, A. Wahab, S. Mahiuddin, W. Kunz and P. Jungwirth, *J. Phys. Chem. B*, 2006, **110**, 15939.

86      Y. Miller, J. L. Thomas, D. D. Kemp, B. J. Finlayson-Pitts, M. S. Gordon, D. J. Tobias and R. B. Gerber, *J. Phys. Chem. A*, 2009, **113**, 12805.

87      M. A. Brown, B. Winter, M. Faubel and J. C. Hemminger, *J. Am. Chem. Soc.*, 2009, **131**, 8354-8355.

88      W. Hua, D. Verreault and H. C. Allen, *J. Phys. Chem. C*, 2014, **118**, 24941-24949.

89      E. S. Shamay and G. L. Richmond, *J. Phys. Chem. C*, 2010, **114**, 12590-12597.

90      R. G. Zepp, J. Hoigne and H. Bader, *Environ. Sci. and Technol.*, 1987, **21**, 443-450.

91      R. Zellner, M. Exner and H. Herrmann, *J Atmos Chem*, 1990, **10**, 411-425.

92      P. Warneck and C. Wurzinger, *J. Phys. Chem.*, 1988, **92**, 6278-6283.

93      H. Herrmann, *Phys. Chem. Chem. Phys.*, 2007, **9**, 3935-3964.

94      P. Nissenson, D. Dabdub, R. Das, V. Maurino, C. Minero and D. Vione, *Atmos. Environ.*, 2010, **44**, 4859.

95      M. Xu, R. Spinney and H. C. Allen, *J. Phys. Chem. B*, 2009, **113**, 4102-4110.

96      L. M. Wingen, A. C. Moskun, S. N. Johnson, J. L. Thomas, M. Roeselova, J. Tobias, D, M. T. Kleinman and B. J. Finlayson-Pitts, *J. Phys. Chem. Chem. Phys.*, 2008, 5668.

97      L. Chu and C. Anastasio, *J. Phys. Chem. A*, 2003, **107**, 9594-9602.

23

98      E. S. Galbavy, K. Ram and C. Anastasio, *J. Photochem. Photobiol. A*, 2010, **209**, 186-192.

99      D. A. Skoog, F. J. Holler and T. A. Nieman, *Principles of Instrumental Analysis, 5th Edition*, Saunders College Publishing, Philadelphia, 1998.

100     I. N. Tang and H. R. Munkelwitz, *J. Geophys. Res.*, 1994, **99**, 18801-18808.

101     A. Verdaguer, G. M. Sacha, M. Luna, D. Frank Ogletree and M. Salmeron, *J. Chem. Phys.*, 2005, **123**, 124703.

102     M. C. Foster and G. E. Ewing, *J. Chem. Phys.*, 2000, **112**, 6817-6826.

103     G. E. Ewing, *Chem. Rev.*, 2006, **106**, 1511-1526.

104     S. Romakkaniemi, K. Hämeri, M. Väkevä and A. Laaksonen, *J. Phys. Chem. A*, 2001, **105**, 8183-8188.

105     P. K. Hudson, J. Schwarz, J. Baltrusaitis, E. R. Gibson and V. H. Grassian, *J. Phys. Chem. A*, 2007, **111**, 544-548.

106     K. B. Benedict, A. S. McFall and C. Anastasio, *Environ. Sci. Technol.*, In preparation.

107     J. Carper, *The CRC Handbook of Chemistry and Physics*, Chemical Rubber Publishing Co., Boca Raton, Fl, 1994.

108     R. H. Stokes and R. A. Robinson, *Ind. Eng. Chem.*, 1949, **2013**.

**Figure 1:** (a) $NO_2$ production during photolysis experiments for aqueous thin films of $Ca(NO_3)_2$ (red, squares), $NaNO_3$ (orange, diamonds), $Mg(NO_3)_2$ (purple, circles), $KNO_3$ (green, diamonds) and $RbNO_3$ (blue, triangles), and (b) the corresponding rates of $NO_2$ production at 298 K in air. Hatched bars and open symbols for $KNO_3$ denote experiments conducted below the DRH. Error bars are 2s of triplicate experiments.
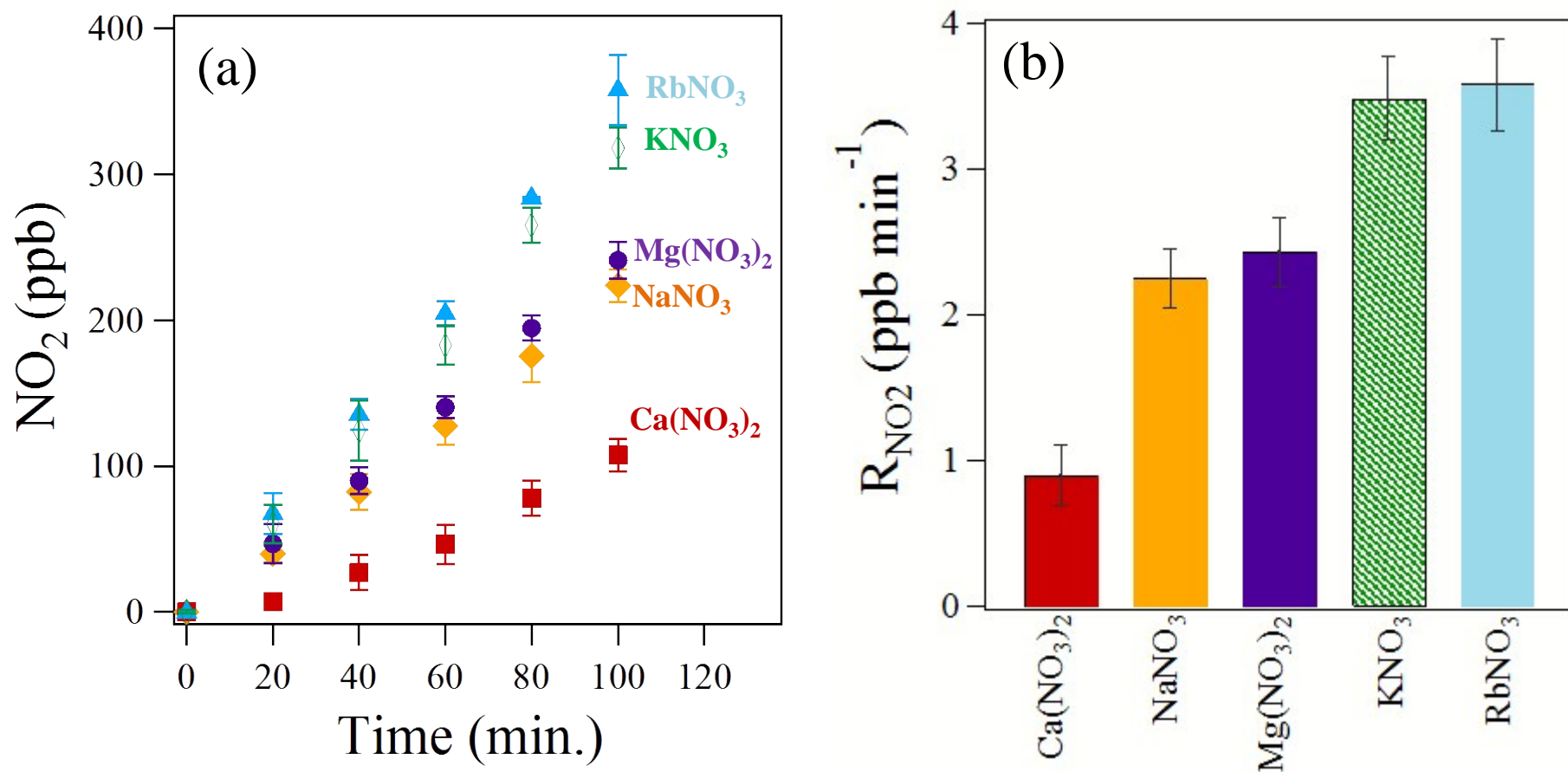
**Figure 2:** Rates of NO$_2$ release in NaNO$_3$ photolysis experiments as a function of RH. The vertical dashed line is the NaNO$_3$ DRH. Error bars are 2s of duplicate experiments.
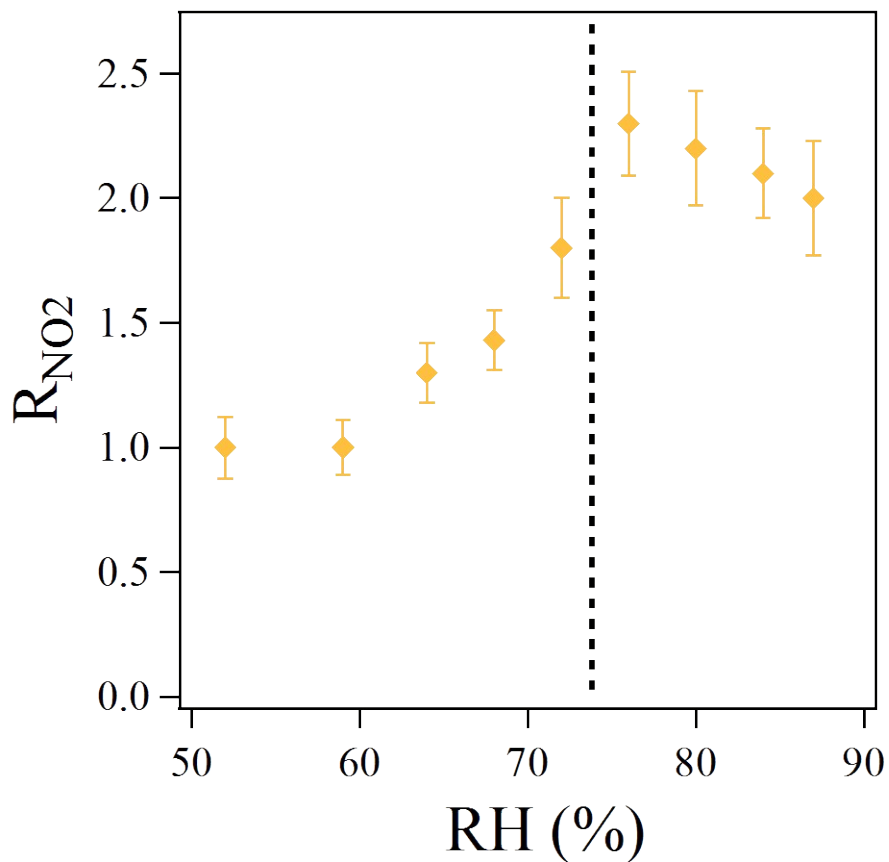
**Figure 3:** The rate of OH production in bulk-phase photolysis studies conducted at 313 nm and 298 K. Error bars are 2s of triplicate experiments.